PAPER

MIMO-OFDM Precoding Technique for Minimizing BER Upper Bound of MLD

Boonsarn PITAKDUMRONGKIJA[†a)], ***Nonmember***, **Kazuhiko FUKAWA**[†], ***Member***, **Hiroshi SUZUKI**[†], ***Fellow***, ***and*** **Takashi HAGIWARA**[††], ***Nonmember***

SUMMARY This paper proposes a new MIMO-OFDM precoding technique that aims to minimize a bit error rate (BER) upper bound of the maximum likelihood detection (MLD) in mobile radio communications. Using a steepest descent algorithm, the proposed method estimates linear precoding matrices that can minimize the upper bound of BER under power constraints. Since the upper bound is derived from all the pairwise error probabilities, this method can effectively optimize overall Euclidean distances between signals received by multiple antennas and their replicas. Computer simulations evaluate the BER performance and channel capacity of the proposed scheme for 2×2 and 4×4 MIMO-OFDM systems with BPSK, QPSK, and 16QAM. It is demonstrated that the proposed precoding technique is superior in terms of average BER to conventional precoding methods including a precoder which maximizes only the minimum Euclidean distance as the worst case.

key words: *mobile communication, MIMO-OFDM, ML detection, precoding, minimum BER, pairwise error*

1. Introduction

The multiple-input multiple-output (MIMO) system has recently attracted much attention because it is one of the most promising techniques to realize high speed mobile communications. A major advantage of the MIMO system is to increase the channel capacity using multiple transmit and receive antennas [1], [2]. The channel capacity can be maximized by the linear precoding technique on the assumption that the channel state information (CSI) is available at the transmitter [2].

Some applications, however, attach importance to the bit error rate (BER) rather than the capacity gain. Therefore, there have been considerable number of researches on the minimum BER (MBER) precoding techniques [3]–[20]. The MBER precoding can be classified into two types: one assumes the linear detection whereas the other assumes the nonlinear detection. As one of the *linear detection type*, the precoder proposed in [3], [4] can minimize the symbol detection error rate of the minimum mean square error (MMSE) detector, and thus approximately achieves the minimum BER. A finite impulse response (FIR) precoder also nearly yields the minimum BER of an FIR filter-type receiver [5], [6]. Under a constraint that BER of the MMSE or zero-forcing (ZF) detectors should be less than a targeted value, a precoder can minimize the total transmit power [7].

These MBER precoders, however, are inefficient when a nonlinear receiver such as the maximum likelihood detector (MLD) is employed. For example, the precoder in [3], [4] orthogonalizes the transmitted signals using the singular value decomposition (SVD) of channel matrices. This orthogonalization cannot optimize Euclidean distances between received signals and their replicas, and thus cannot minimize BER of MLD, which highly depends on the overall Euclidean distances.

As the *nonlinear detection type*, some precoders aim to minimize BER of V-BLAST or QR decomposition based detectors [8], [9]. However, these precoders cannot minimize BER when MLD is employed. Another approach maximizes the minimum Euclidean distance when MLD is employed [10]–[12]. The precoder proposed in [10] maximizes a lower bound of the minimum distance by optimizing the smallest singular value of the equivalent channel matrix including the precoding matrix. The precoder in [11] approximately achieves such maximization, whereas one in [12] exactly does. Although these minimum distance-based precoders are simple to implement, they cannot achieve significant improvement in BER over the spatial multiplexing because they do not directly minimize BER bounds. In fact, their BER performance is found to be only slightly better than that of the maximum-SNR transmission scheme proposed in [13].

On the other hand, the MBER precoder for MLD that is robust to CSI imperfection at the transmitter has been proposed in [14]. Its cost function is derived from the pairwise error probability similar to the technique used in [15]. However, the precoding matrix is still assumed to have the same structure as that of the precoder for the linear detector. Thus its improvement in average BER over the spatial multiplexing is expected to be small. Note that other precoding schemes that optimize the transmission diversity can maximize the average SNR, and thus are out of the scope of the instantaneous precoding scenarios [16]–[20]. It is also noteworthy that the MBER precoding seems to be similar to the MBER beamforming in [21] but is different from this, because the latter obtains the optimum weight vector of the diversity combining at the receiver under MBER.

This paper proposes a new MIMO-OFDM precoding method that minimizes BER of MLD. To optimize the Euclidean distance effectively, the proposed method controls the precoding matrices by minimizing an upper bound of

Manuscript received September 25, 2007.

[†]The authors are with Tokyo Institute of Technology, Tokyo, 152-8550 Japan.

[††]The author was formerly with Tokyo Institute of Technology, Tokyo, 152-8550 Japan.

a) E-mail: boonju@radio.ss.titech.ac.jp

DOI: 10.1093/ietcom/e91–b.7.2287

Copyright © 2008 The Institute of Electronics, Information and Communication Engineers

BER based on the pairwise error. The rest of the paper is organized as follows. In Sect. 2, a MIMO-OFDM system employing the precoder is described. The proposed MBER precoding is derived in Sect. 3. In Sect. 4, the performances of the proposed and conventional precoding schemes are evaluated by computer simulations. Finally, the conclusion remarks are given in Sect. 5.

2. System Model

2.1 Transmitter

Consider a MIMO-OFDM system with N_T transmit and N_R receive antennas shown in Fig. 1. Let N and M denote the total number of subcarriers and the number of data streams to be transmitted by each subcarrier, respectively. It is assumed that $M \leq \min\{N_T, N_R\}$.

Figure 1(a) shows a block diagram of the transmitter. The information bits are divided into N groups of M bit streams and passed into the modulators. Then the N_T-by-M precoder matrix transforms M modulated signals into N_T transmitted signals for each subcarrier. Finally, N groups of N_T transmitted signals are separated and passed into the corresponding IFFT and Guard Interval (GI) insertion processors. The input signal of the IFFT processor corresponding to the k-th ($1 \leq k \leq N_T$) transmit antenna, the n-th ($0 \leq n \leq N-1$) subcarrier, and the i-th symbol, is denoted by $s_k(n, i)$ and is expressed as

$$s_k(n, i) = \sum_{m=1}^{M} F_{km}(n) b_m(n, i), \tag{1}$$

where $F_{km}(n)$ is the (k, m)-th element of the n-th subcarrier precoding matrix and $b_m(n, i)$ is the modulation signal of the m-th ($1 \leq m \leq M$) data stream at the n-th subcarrier in the i-th symbol. $b_m(n, i)$ is assumed to have the following property:

$$\langle b^*_{m_1}(n_1, i_1) b_{m_2}(n_2, i_2) \rangle = \delta_{m_1 m_2} \delta_{n_1 n_2} \delta_{i_1 i_2}, \tag{2}$$

where $\langle\ \rangle$ and * denote the ensemble average and complex conjugation, respectively. δ_{ij} is the Kronecker delta.

For vector notation, an N_T-by-1 transmitted signal vector $\mathbf{s}(n, i)$, an N_T-by-M precoding matrix $\mathbf{F}(n)$, and an M-by-1 modulation signal vector $\mathbf{b}(n, i)$ are defined as

$$\mathbf{s}^{\mathrm{H}}(n, i) = \left[s^*_1(n, i) \ \ldots \ s^*_{N_T}(n, i) \right], \tag{3}$$

$$(\mathbf{F}(n))_{km} = F_{km}(n), \tag{4}$$

$$\mathbf{b}^{\mathrm{H}}(n, i) = \left[b^*_1(n, i) \ \ldots \ b^*_M(n, i) \right], \tag{5}$$

where the superscript ^{H} denotes Hermitian transposition. Then, the transmitted signal of (1) can be rewritten as

$$\mathbf{s}(n, i) = \mathbf{F}(n) \mathbf{b}(n, i). \tag{6}$$

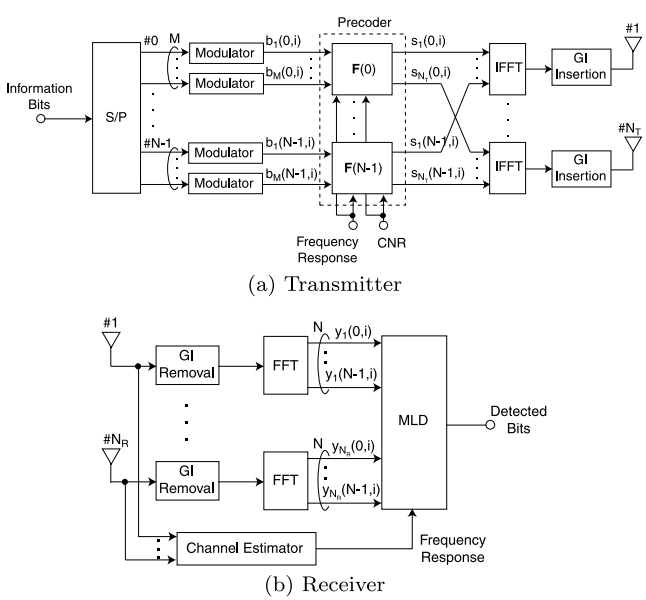

Fig. 1 MIMO-OFDM system.

2.2 Receiver

The receiver uses the N_R antennas to receive signals as shown in Fig. 1(b). On the assumption that the channel frequency response remains constant during one OFDM symbol and that the maximum delay time of propagation paths does not exceed the GI duration, the FFT output of the signal received by the l-th ($1 \leq l \leq N_R$) receive antenna at the n-th subcarrier in the i-th symbol is denoted by $y_l(n, i)$, and is given by

$$y_l(n, i) = \sum_{k=1}^{N_T} H_{lk}(n) s_k(n, i) + z_l(n, i), \tag{7}$$

where $H_{lk}(n)$ represents the channel frequency response at the n-th subcarrier between the k-th transmit and the l-th receive antennas, and $z_l(n, i)$ is an FFT output of the additive white Gaussian noise (AWGN) with zero mean. The autocorrelation of $z_l(n, i)$ is given by

$$\langle z^*_{l_1}(n_1, i_1) z_{l_2}(n_2, i_2) \rangle = \sigma^2_N \delta_{l_1 l_2} \delta_{n_1 n_2} \delta_{i_1 i_2}, \tag{8}$$

where σ^2_N is the average power of $z_l(n, i)$. Substituting (1) into (7) yields

$$y_l(n, i) = \sum_{k=1}^{N_T} H_{lk}(n) \sum_{m=1}^{M} F_{km}(n) b_m(n, i) + z_l(n, i). \tag{9}$$

For vector notation, an N_R-by-1 received signal vector $\mathbf{y}(n, i)$, an N_R-by-N_T channel frequency response matrix $\mathbf{H}(n)$, and an N_R-by-1 noise vector $\mathbf{z}(n, i)$ are defined as

$$\mathbf{y}^{\mathrm{H}}(n, i) = \left[y^*_1(n, i) \ \ldots \ y^*_{N_R}(n, i) \right], \tag{10}$$

$$(\mathbf{H}(n))_{lk} = H_{lk}(n), \tag{11}$$

$$\mathbf{z}^{\mathrm{H}}(n, i) = \left[z^*_1(n, i) \ \ldots \ z^*_{N_R}(n, i) \right]. \tag{12}$$

Using these vectors and matrix, the received signals of (9) can be rewritten in a vector form as

$$\mathbf{y}(n,i) = \mathbf{H}(n)\mathbf{F}(n)\mathbf{b}(n,i) + \mathbf{z}(n,i). \tag{13}$$

The receiver employs MLD for signal detection. Therefore, the estimate of $\mathbf{b}(n,i)$ is given by

$$\tilde{\mathbf{b}}(n,i) = \arg\min_{\hat{\mathbf{b}}(n,i)} \left\|\mathbf{y}(n,i) - \tilde{\mathbf{H}}(n)\tilde{\mathbf{F}}(n)\hat{\mathbf{b}}(n,i)\right\|^2, \tag{14}$$

where $\tilde{\mathbf{b}}(n,i)$ denotes the estimate of $\mathbf{b}(n,i)$, $\hat{\mathbf{b}}(n,i)$ represents a candidate of $\mathbf{b}(n,i)$, and $\tilde{\mathbf{H}}(n)$ and $\tilde{\mathbf{F}}(n)$ are the estimates of the channel frequency response matrix and the precoding matrix, respecively. $\|\ \|$ denotes the vector norm. This paper assumes that $\mathbf{H}(n)$ and $\mathbf{F}(n)$ are perfectly known to the receiver, thus $\tilde{\mathbf{H}}(n) = \mathbf{H}(n)$ and $\tilde{\mathbf{F}}(n) = \mathbf{F}(n)$.

3. MBER Criterion Precoding

3.1 Derivation of Pairwise Error Probability

Suppose that $\mathbf{b}(n,i)$ is transmitted and that $\mathbf{c}(n,i)$ is a candidate different from $\mathbf{b}(n,i)$. The detector performs erroneous detection and determines that $\mathbf{c}(n,i)$ rather than $\mathbf{b}(n,i)$ is transmitted if the following inequality holds:

$$\begin{aligned}&\|\mathbf{y}(n,i) - \mathbf{H}(n)\mathbf{F}(n)\mathbf{b}(n,i)\|^2 \\ &\quad > \|\mathbf{y}(n,i) - \mathbf{H}(n)\mathbf{F}(n)\mathbf{c}(n,i)\|^2 .\end{aligned} \tag{15}$$

Substituting (13) into (15) results in

$$\begin{aligned}&\|\mathbf{H}(n)\mathbf{F}(n)\left[\mathbf{b}(n,i) - \mathbf{c}(n,i)\right]\|^2 \\ &\quad +2\Re\left\{\mathbf{z}^{\mathrm{H}}(n,i)\mathbf{H}(n)\mathbf{F}(n)\left[\mathbf{b}(n,i) - \mathbf{c}(n,i)\right]\right\} < 0\end{aligned} \tag{16}$$

For simplicity, scalars ζ and η are defined as

$$\zeta = \|\mathbf{H}(n)\mathbf{F}(n)\left[\mathbf{b}(n,i) - \mathbf{c}(n,i)\right]\|^2 , \tag{17}$$

$$\eta = \mathbf{z}^{\mathrm{H}}(n,i)\mathbf{H}(n)\mathbf{F}(n)\left[\mathbf{b}(n,i) - \mathbf{c}(n,i)\right] . \tag{18}$$

Therefore, (16) can be rewritten as

$$2\Re\left\{\eta\right\} < -\zeta. \tag{19}$$

Since η is a linear combination of $z_l^*(n,i)$, η is a complex Gaussian random variable with zero mean and variance σ_η^2 that is given by

$$\sigma_\eta^2 = \sigma_N^2\zeta. \tag{20}$$

Let $\tilde{b} = \{b_m(n,i) \mid 1 \le m \le M\}$ and $\mathcal{H} = \{H_{lk}(n) \mid 1 \le l \le N_R,\ 1 \le k \le N_T\}$. $\tilde{c}$ is defined in the same way as $\tilde{b}$. From (19) and (20), the pairwise error probability that $\tilde{c}$ rather than $\tilde{b}$ is detected, given the channel frequency response $\mathcal{H}$, is derived as

$$\begin{aligned}P(\tilde{b} \to \tilde{c}\,|\mathcal{H}) &= P\left(2\Re\left\{\eta\right\} < -\zeta\,|\mathcal{H}\right) \\ &= \frac{1}{\sqrt{4\pi\sigma_\eta^2}}\int_{-\infty}^{-\zeta} e^{-x^2/4\sigma_\eta^2}\,dx = \frac{1}{2}\mathrm{erfc}\sqrt{\gamma(\tilde{b} \to \tilde{c})},\end{aligned} \tag{21}$$

where $\mathrm{erfc}(x)$ denotes the complementary error function and $\gamma(\tilde{b} \to \tilde{c})$ is defined as

$$\gamma(\tilde{b} \to \tilde{c}) = \frac{\zeta}{4\sigma_N^2}. \tag{22}$$

Applying the Chernoff bound to (21) yields an upper bound of this pairwise error probability as

$$P(\tilde{b} \to \tilde{c}\,|\mathcal{H}) \le \exp[-\gamma(\tilde{b} \to \tilde{c})]. \tag{23}$$

3.2 Transmit Power Constraints

The total average transmit power P_0 is given by

$$P_0 = \sum_{n=0}^{N-1}\mathrm{tr}\left\{\langle\mathbf{s}(n,i)\mathbf{s}^{\mathrm{H}}(n,i)\rangle\right\} = \sum_{n=0}^{N-1}\mathrm{tr}\left\{\mathbf{F}(n)\mathbf{F}^{\mathrm{H}}(n)\right\}, \tag{24}$$

where tr{ } denotes the trace and the derivation used (2). $\mathbf{F}(n)$ should satisfy (24) under a constraint that P_0 is constant. In addition, when each transmit amplifier limits the power of its input signal, the following constraint of equal transmit power for each antenna is imposed:

$$\sum_{n=0}^{N-1}\left(\mathbf{F}(n)\mathbf{F}^{\mathrm{H}}(n)\right)_{kk} = P_0/N_T \quad \text{for } 1 \le k \le N_T. \tag{25}$$

3.3 Criterion and Steepest Descent Algorithm

From the pairwise error probability of (21), an upper bound on the bit error rate can be obtained as

$$P_e \le \sum_n \frac{1}{N}\sum_{\tilde{b}} P(\tilde{b})\sum_{\tilde{c}\neq\tilde{b}}\frac{N_e(\tilde{b} \to \tilde{c})}{N_b}P(\tilde{b} \to \tilde{c}\,|\mathcal{H}), \tag{26}$$

where the summations take place over all the subcarriers, modulation signals, and erroneous signals. $N_e(\tilde{b} \to \tilde{c})$ denotes the number of error bits when the detected signal is not $\tilde{b}$ but $\tilde{c}$, N_b is the total number of transmitted bits in $\tilde{b}$, and $P(\tilde{b})$ is the probability that $\tilde{b}$ is transmitted.

Note that the minimum distance-based precoder in [12] takes only reduced summation over a subset of $\tilde{c}$ that gives the smallest Euclidean distance. Therefore, it can only minimize a much looser bound of BER than the bound of (26).

On the assumption that BER at each subcarrier is statistically independent of each other and that every symbol is equally probable, the bound on the bit error rate for the n-th subcarrier in (26) can be simplified as

$$P_e \le \sum_n P_e(n), \tag{27}$$

$$P_e(n) = \frac{P(\tilde{b})}{2N_bN}\sum_{\tilde{b}}\sum_{\tilde{c}\neq\tilde{b}} N_e(\tilde{b} \to \tilde{c})\mathrm{erfc}\sqrt{\gamma(\tilde{b} \to \tilde{c})}, \tag{28}$$

where (21) was used and $P(\tilde{b})$ is constant irrespectively of $\tilde{b}$. From (28), the minimum BER (MBER) precoding matrix

can be obtained by solving the following set of nonlinear equations:

$$\mathbf{F}(n) = \arg\min_{\hat{\mathbf{F}}(n)} P_e(n),\ 0 \le n \le N-1, \tag{29}$$

under the power constraints of (24) or (25). Here, $\hat{\mathbf{F}}(n)$ is a precoding matrix candidate of $\mathbf{F}(n)$. Since the direct solution to (29) is rather complicated, this paper applies the gradient based method, namely the steepest descent algorithm.

The cost function for the steepest descent algorithm is obtained from (28) and is defined as

$$J_e(\mathbf{F}(n)) = \sum_{\tilde{b}} \sum_{\tilde{c} \ne \tilde{b}} N_e(\tilde{b} \to \tilde{c}) \mathrm{erfc} \sqrt{\gamma(\tilde{b} \to \tilde{c})}. \tag{30}$$

The conjugate derivative of (30) with respect to $\mathbf{F}(n)$ is given by

$$\begin{aligned}\frac{\partial J_e(\mathbf{F}(n))}{\partial \mathbf{F}^*(n)} &= -\frac{\mathbf{H}^{\mathrm{H}}(n)\mathbf{H}(n)\mathbf{F}(n)}{4\sqrt{\pi}\sigma_N^2} \\ &\times \sum_{\tilde{b}} \sum_{\tilde{c} \ne \tilde{b}} N_e(\tilde{b} \to \tilde{c}) \mathbf{A}(\tilde{b} \to \tilde{c}) \\ &\times [\gamma(\tilde{b} \to \tilde{c})]^{-1/2} \exp[-\gamma(\tilde{b} \to \tilde{c})],\end{aligned} \tag{31}$$

where the M-by-M matrix $\mathbf{A}(\tilde{b} \to \tilde{c})$ is defined as

$$\begin{aligned}\mathbf{A}(\tilde{b} \to \tilde{c}) &= [\mathbf{b}(n,i) - \mathbf{c}(n,i)] \\ &\times [\mathbf{b}(n,i) - \mathbf{c}(n,i)]^{\mathrm{H}}.\end{aligned} \tag{32}$$

The derivation of (31) is given in Appendix A. Thus, the steepest descent algorithm for obtaining the MBER precoding matrix is formulated as follows.

1. Calculate a new precoding matrix using the following update equation:

$$\begin{aligned}\tilde{\mathbf{F}}^{(q)}(n) &= \mathbf{F}^{(q-1)}(n) - \mu \left.\frac{\partial J_e(\mathbf{F}(n))}{\partial \mathbf{F}^*(n)}\right|_{\mathbf{F}^{(q-1)}(n)} \\ &\text{for } 0 \le n \le N-1,\end{aligned} \tag{33}$$

   where q denotes an iteration index, $\mathbf{F}^{(q)}(n)$ is the q-th guess of $\mathbf{F}(n)$, and μ is a positive value that affects the convergence of the algorithm.
2. Normalize the newly computed precoding matrix so that the power constraint of (24) can be satisfied

$$\alpha = \sum_{n=0}^{N-1} \mathrm{tr}\left\{\tilde{\mathbf{F}}^{(q)}(n)\tilde{\mathbf{F}}^{(q)^{\mathrm{H}}}(n)\right\}/P_0, \tag{34}$$

$$\mathbf{F}^{(q)}(n) = \alpha^{-1/2}\tilde{\mathbf{F}}^{(q)}(n). \tag{35}$$

   When the constraint of (25) is imposed instead of (24), the normalization is modified as

$$\mathbf{f}_k^{(q)}(n) = \left[F_{k1}^{(q)}(n)\ \ldots\ F_{kM}^{(q)}(n)\right], \tag{36}$$

$$\tilde{\mathbf{f}}_k^{(q)}(n) = \left[\tilde{F}_{k1}^{(q)}(n)\ \ldots\ \tilde{F}_{kM}^{(q)}(n)\right], \tag{37}$$

$$\alpha = \sum_{n=1}^{N} \left(\tilde{\mathbf{F}}^{(q)}(n)\tilde{\mathbf{F}}^{(q)^{\mathrm{H}}}(n)\right)_{kk} / (P_0/N_T), \tag{38}$$

$$\mathbf{f}_k^{(q)}(n) = \alpha^{-1/2}\tilde{\mathbf{f}}_k^{(q)}(n) \tag{39}$$

   for $1 \le k \le N_T$.
3. Repeat step 1 and 2 until the number of iterations exceeds a predetermined number or $\partial J_e(\mathbf{F}(n))/\partial \mathbf{F}^*(n)$ becomes nearly equal to zero.
   Note that the conventional MBER precoder in [14] assumes that its precoding matrix structure is similar to that of the linear receiver and can be expressed as $\mathbf{F}(n) = \mathbf{V}(n)\mathbf{\Phi}(n)\mathbf{T}$, where $\mathbf{V}(n)$ is an N_T-by-M right singular vector matrix of $\mathbf{H}(n)$, $\mathbf{\Phi}(n)$ is an M-by-M positive-valued diagonal matrix, and $\mathbf{T}$ is an M-by-M DFT matrix. The steepest descent algorithm in [14] controls only $\mathbf{\Phi}(n)$ rather than $\mathbf{F}(n)$.

On the other hand, the steepest descent algorithm for the Chernoff bound of (23) can also be derived. Similarly, the cost function is defined as

$$J_c(\mathbf{F}(n)) = \sum_{\tilde{b}} \sum_{\tilde{c} \ne \tilde{b}} N_e(\tilde{b} \to \tilde{c}) \exp[-\gamma(\tilde{b} \to \tilde{c})]. \tag{40}$$

The conjugate derivative of (40) is given by

$$\begin{aligned}\frac{\partial J_c(\mathbf{F}(n))}{\partial \mathbf{F}^*(n)} &= -\frac{\mathbf{H}^{\mathrm{H}}(n)\mathbf{H}(n)\mathbf{F}(n)}{4\sigma_N^2} \\ &\times \sum_{\tilde{b}} \sum_{\tilde{c} \ne \tilde{b}} N_e(\tilde{b} \to \tilde{c}) \mathbf{A}(\tilde{b} \to \tilde{c}) \\ &\times \exp[-\gamma(\tilde{b} \to \tilde{c})].\end{aligned} \tag{41}$$

The rests of the algorithm follow the same steps as those of the complementary error function.

The initial value $\mathbf{F}^{(0)}(n)$ of the precoding matrix is set to an equally weighted diagonal matrix, which initially results in equal power distribution among transmit antennas. Moreover, the step size parameter μ decreases linearly with q in order to obtain a good convergence characteristic [22]. The verifications of the initialization and the step size adaptation will be given in the simulation result section.

Note that this paper considers only uncoded systems. However, the proposed precoder is also applicable to coded systems and is expected to improve BER of a receiver employing the turbo equalization. The turbo equalization process is briefly described in Appendix B and its theoretical framework can be found in [23]. Since the proposed precoder minimizes the detection error probability of the signal detector, its output becomes more reliable. Then, such highly reliable output is further used for decoding, and thus the average BER of the overall system is expected to improve.

Table 1 N_γ required for each subcarrier per iteration.

Modulation	Number of Data Stream	
	$M = 2$	$M = 4$
BPSK	12	240
QPSK	240	65,280
16QAM	65,280	4.295×10^9

Table 2 $N_{\gamma c}$ required for each subcarrier.

Modulation	Number of Data Stream	
	$M = 2$	$M = 4$
BPSK	9.6×10^3	2.4×10^5
QPSK	9.6×10^4	$> 2.611 \times 10^7$
16QAM	6.528×10^6	$> 4.295 \times 10^{11}$

Table 3 Simulation parameters.

Modulation	QPSK (16QAM)
Number of Antenna ($N_T \times N_R$)	2×2 (4×4 : BPSK)
Data Stream M	2 (4 : BPSK)
Effective OFDM Subcarrier	52 (Pilot : 4, Data : 48)
Subcarrier Spacing	312.5 kHz
GI Length	0.8 μs
Symbol Length (Including GI)	4.0 μs
No. of FFT point N	64
Channel Model	17-Path Exponential Decay Rayleigh Fading
Maximum Doppler Frequency	0 Hz
CSI at Transmitter	Ideal
CSI at Receiver	Ideal
Signal Detection	MLD

3.4 Complexity of Optimization Process

The steepest descent algorithm calculates the conjugate derivative of (31) or (41) for each subcarrier at every iteration. Much of the complexity arises from the calculation of $\gamma(\tilde{b} \to \tilde{c})$, which involves many complex matrix operations. Therefore, the complexity can be evaluated in terms of the number of $\gamma(\tilde{b} \to \tilde{c})$ required for each subcarrier. Let S be the number of modulation constellation points, and let N_γ denote the number of $\gamma(\tilde{b} \to \tilde{c})$ required for each subcarrier per iteration, which is equal to the number of the summation over $\tilde{b}$ and $\tilde{c}$ and is given by

$$N_\gamma = S^M(S^M - 1). \tag{42}$$

The total number of $\gamma(\tilde{b} \to \tilde{c})$ required for each subcarrier is given by

$$N_{\gamma c} = N_c N_\gamma = N_c S^M(S^M - 1). \tag{43}$$

where N_c denotes the minimum iteration number to guarantee sufficient convergence.

Table 1 shows N_γ for BPSK, QPSK and 16QAM with M equal to two and four. Table 2 shows $N_{\gamma c}$, where values of N_c were determined by a preparatory computer simulation that employed the most suitable value of μ when the maximum number of iterations was set to 1,000. State-of-the-art PCs require excessive computational time for the performance evaluation when $N_{\gamma c}$ is larger than 10^7.

4. Simulation Results

4.1 Simulation Conditions

Computer simulations were conducted to verify the performance of the proposed precoding method. Simulation parameters are summarized in Table 3. The OFDM packet format follows the IEEE 802.11a standard [24]. It was assumed that the ideal CSI is available at both the transmitter and receiver. The receiver uses MLD for the signal detection. As initial values of $\{\mathbf{F}(n)|0 \le n \le N-1\}$, those of the unweighted MMSE precoding [3] and the equally weighted diagonal matrix were investigated. The average BER bound was evaluated from (26), and the cost functions of (30) and (40) are indicated by J_e and J_c, respectively. Note that SNR and E_b/N_0 in the following graphs are those per receive antenna of the spatial multiplexing which does not perform any precoding.

The main part of the simulation in Sects. 4.2–4.4 clarifies various performances of the conventional and proposed MBER precoders with a 2×2 MIMO-OFDM system, $M = 2$, and QPSK modulation. Sect. 4.5 shows the performance in more complicated systems; $M = 4$ or 16QAM as indicated in the parentheses of Table 3. Since the $N_{\gamma c} > 10^7$ case requires excessive simulation time, Table 2 explains the reason for the limited demonstration of only $M = 4$ with BPSK and $M = 2$ with 16QAM. Nevertheless, the results will give insights to the $M > 4$ case with higher modulation order.

4.2 Convergence Characteristics

4.2.1 Step Size

Figure 2 shows the effect of the step size on the average BER bound, where the total power constraint of (24) and the equal transmit power constraint of (25) are imposed on (a) and (b), respectively. Average $E_b/N_0 = 12$ dB, and the maximum number of iterations of the steepest descent algorithm was set to 1,000. With both the constraints, the equal power initialization is superior in the average BER bound to the MMSE precoding initialization. The performance of the equal power initialization with the equal transmit power constraint is almost the same as that with the total power constraint. On the other hand, the MMSE precoding initialization with the equal transmit power constraint can bring about a slight improvement over that with the total power constraint, when the step size is nearly equal to 10^{-3}.

4.2.2 Iteration Number

Figure 3(a) shows convergence characteristics of several variations of the steepest descent algorithm with the total power constraint. Two schemes of step size adaptation are

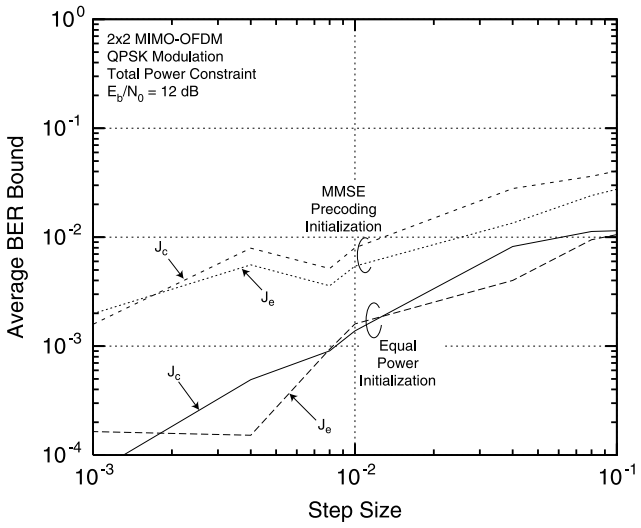

(a) Total power constraint

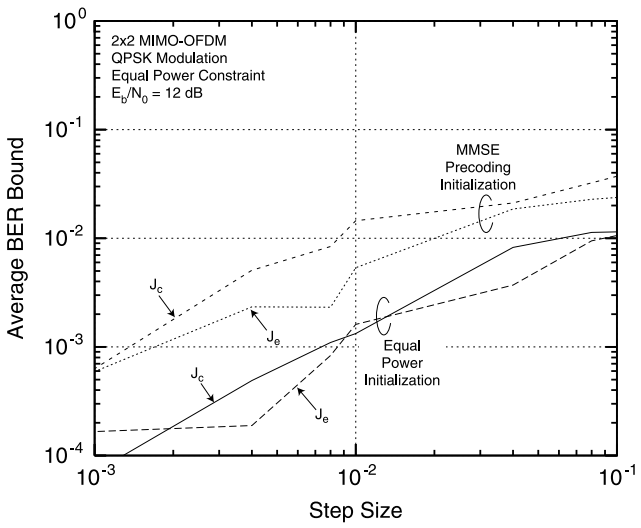

(b) Equal transmit power constraint

Fig. 2 Average BER bound vs. step size.

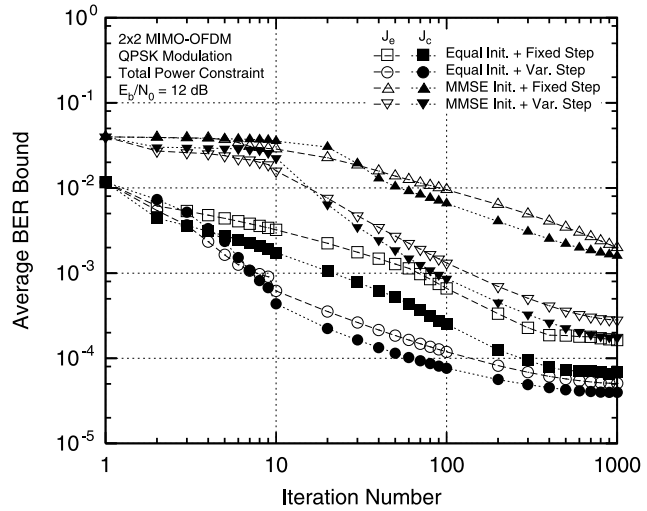

(a) Total power constraint

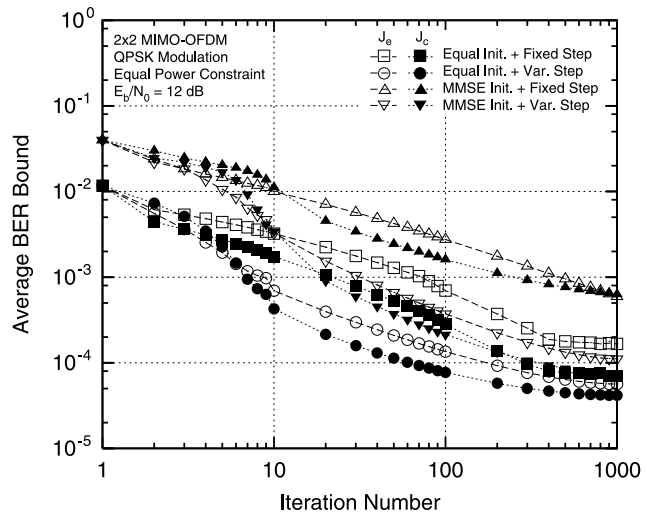

(b) Equal transmit power constraint

Fig. 3 Average BER bound vs. iteration number.

applied. One is the fixed step size scheme, which fixes μ to 1.0×10^{-3} throughout the gradient method iteration. The other is the variable step size scheme, which reduces the value of μ from 1.0×10^{-1} to 1.0×10^{-3} linearly with the iteration. It can be seen that the gradient method using the equal power initialization outperforms that using the MMSE precoding initialization when the step size is fixed to 1.0×10^{-3}. In addition, the variable step size scheme outperforms the fixed step size scheme for all the initialization methods. Furthermore, the gradient method employing J_c with the equal power initialization and the variable step size scheme shows the best convergence characteristic. It should be noted that J_c outperforms J_e because the term $[\gamma(\tilde{b} \to \tilde{c})]^{-1/2}$ in (31) makes the gradient of J_e smaller than that of J_c of (41) at high SNRs, and then makes the convergence rate of J_e slower than that of J_c.

Figure 3(b) shows the convergence characteristics with the equal transmit power constraint. It can be seen from Figs. 3(a) and (b) that the algorithm using the MMSE precoding initialization with the equal transmit power constraint outperforms that with the total power constraint. However, there is no significant difference in the BER bound of the equally weighted diagonal matrix initialization between the two constraints. Thus, it can be inferred that the equal power initialization converges to the same local minimum regardless of the constraint. Moreover, it can be seen that the average BER bound converges sufficiently at 400 iterations in the case of J_c with the equal power initialization and the variable step size.

4.3 Average BER Performance

Figure 4 shows average BER performances of the following MIMO-OFDM transmission schemes: the spatial multiplexing, the waterfilling precoding, the unweighted MMSE precoding, the minimum distance-based precoding, the conventional MBER precoding, and the proposed MBER precod-

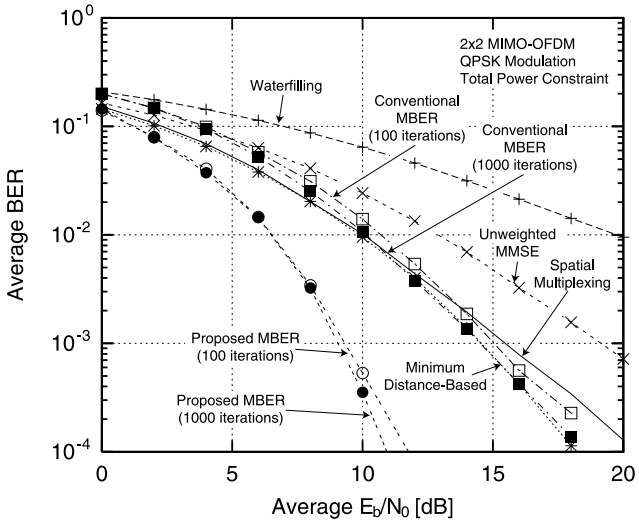

Fig. 4 Average BER performances.

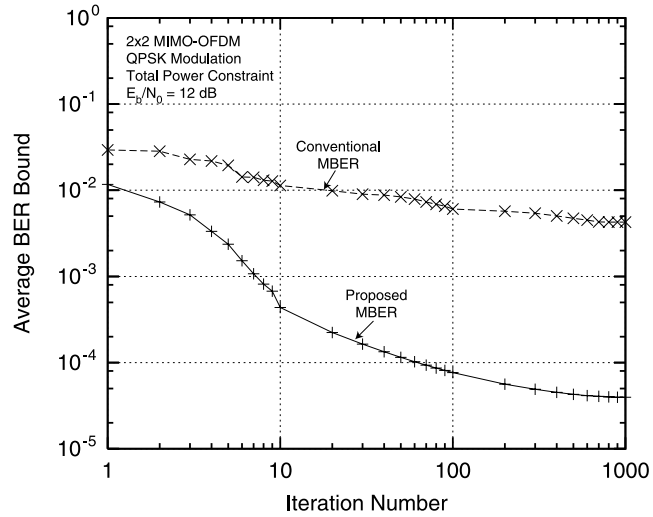

Fig. 5 Convergence characteristics of the conventional and proposed MBER precoders.

ing. Note that the spatial multiplexing does not perform precoding and distributes the power among transmit antennas uniformly. The waterfilling precoder maximizes the channel capacity, while the unweighted MMSE one minimizes BER of the MMSE detector [3]. On the other hand, the minimum distance-based precoder maximizes only the minimum Euclidean distance [12]. The conventional MBER precoding proposed in [14] assumes that its precoding matrix has a structure similar to the solution of the weighted MMSE precoder, and it employs the steepest descent algorithm to optimize the precoding matrix. The proposed MBER precoder uses J_c as its cost function with both the equal power initialization and the variable step size. The average BER performances of the conventional and proposed MBER precoders were evaluated at 100 and 1,000 iterations to show intermediate and sufficient convergence, respectively, and their convergence characteristics are shown in Fig. 5. All schemes adopted the total power constraint.

It can be seen that although the unweighted MMSE precoding can achieve a large improvement over the waterfilling scheme, it is still inferior to the spatial multiplexing. The minimum distance-based and conventional MBER precoding schemes gain a slight improvement over the spatial multiplexing with high SNR. The performance gain of the conventional MBER precoder in average E_b/N_0 is about 1 dB when the number of iterations increases from 100 to 1,000. The proposed MBER precoder produces an improvement of about 7 dB in the average E_b/N_0 at BER = 10^{-3} over the spatial multiplexing, when the maximum number of iterations is 100. When the maximum number of iterations increases from 100 to 1,000, an additional E_b/N_0 improvement of 0.5 dB can be obtained at BER = 10^{-3}. Note that this paper aims to compare the conventional and proposed schemes when their precoding matrices are nearly equal to the optimum values. Therefore, the following simulations set the maximum iteration to 1,000 for both the schemes. Evidently from Fig. 4, the proposed scheme

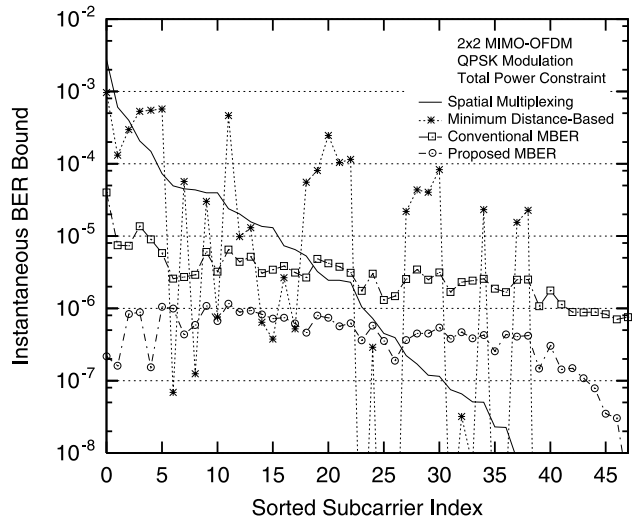

Fig. 6 Distribution of BER bound among subcarriers.

achieves about 6 dB gain of E_b/N_0 over the conventional one at BER = 10^{-3}.

4.4 Effects of MBER Precoding

4.4.1 BER Bound Distribution and Received Signal Replica Constellation

Figure 6 shows the BER bound distribution among subcarriers of some MIMO-OFDM transmission schemes over a specific channel. Only the minimum distance-based, the conventional, and the proposed MBER precoders were evaluated because they are based on the similar criteria involving the Euclidean distance and the probability of error. Note that the BER bound of each subcarrier was calculated from (28) at E_b/N_0 = 12 dB, and that of the spatial multiplexing was chosen as a reference and rearranged in descending or-

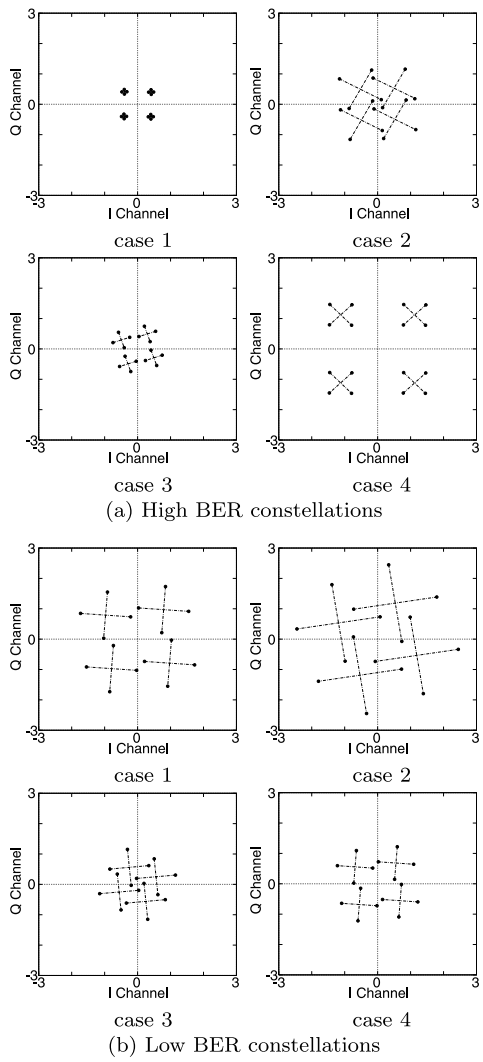

Fig. 7 Signal constellations — case 1: Spatial multiplexing, case 2: Minimum distance-based precoding, case 3: Conventional MBER precoding, and case 4: proposed MBER precoding.

der. Since the minimum distance-based precoder minimizes only a lower bound of BER determined by the minimum Euclidean distance, the improvement of the overall performance cannot be guaranteed. This results in unpredictable BER improvement at each subcarrier as shown. On the other hand, both the conventional and proposed MBER precoders tend to equalize the bound of all subcarriers, and the latter can provide a lower average BER bound than the former does.

Figure 7 shows received signal replicas at one of the receive antennas, where (a) and (b) correspond to the high BER constellations and the low BER constellations, respectively. Note that the high and low BER constellations indicate subcarriers which yield the maximum and minimum BER bounds of the spatial multiplexing system, respectively. With the high BER constellation, the received signal replicas originally have a very small minimum Euclidean distance as shown in Fig. 7(a)-case 1. A slight improvement of the minimum Euclidean distance can be obtained by the minimum distance-based and conventional MBER precoders as shown in Figs. 7(a)-case 2 and case 3, respectively. On the other hand, the proposed MBER precoder can achieve the most desirable constellation as shown in Fig. 7(a)-case 4.

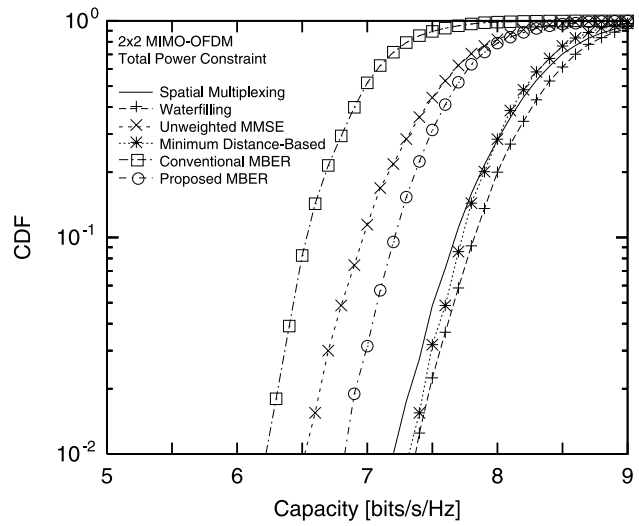

Fig. 8 Outage probability of various MIMO-OFDM systems.

Figure 7(b)-case 1 shows the low BER constellation of the spatial multiplexing. The minimum distance-based precoder tends to improve the minimum Euclidean distance further as shown in Fig. 7(b)-case 2. On the other hand, the conventional and proposed MBER precoders tend to reduce the size of the constellations as shown in Figs. 7(b)-case 3 and case 4, respectively. The reason is as follows. Transmit powers of subcarriers under good channel conditions can be reduced, because such subcarriers can maintain sufficient BER even with reduced powers and the residual powers are distributed to subcarriers under bad channel conditions so that they can improve BER performance. Figures 7(a)-case 4 and 7(b)-case 4 confirm this explanation.

4.4.2 Outage Probability

Figure 8 shows the outage probability (CDF) versus the instantaneous capacity of each MIMO-OFDM transmission scheme with SNR = 15 dB. The instantaneous capacity can be expressed as [1]

$$C = \frac{1}{N}\sum_{n=0}^{N-1}\log_2\det\left[\mathbf{I} + \frac{\mathbf{H}(n)\mathbf{F}(n)\mathbf{F}^{\mathrm{H}}(n)\mathbf{H}^{\mathrm{H}}(n)}{\sigma_N^2}\right] \quad \text{[bits/s/Hz]}, \tag{44}$$

where $\mathbf{I}$ is the N_R-by-N_R identity matrix. Evidently, the waterfilling and the spatial multiplexing outperform the proposed MBER precoding because they can maximize the capacity when CSI is available and unavailable at the transmitter, respectively [2]. Note that the proposed method

aims to minimize BER of a fixed modulation scheme unlike the waterfilling that presumes the adaptive modulation. Surprisingly, the minimum distance-based precoder has the performance close to that of the waterfilling at low outage probability. This is because the minimum distance-based precoder has two modes and can avoid signal transmission over relatively bad channels by adjusting transmit powers, in the same way as the waterfilling [12]. On the other hand, the proposed MBER precoder is superior to the unweighted MMSE and the conventional scheme in the outage capacity at low cumulative probability. The reason is that the proposed precoder can achieve lower average BER, which improves the channel capacity more than the unweighted MMSE and the conventional MBER precoder.

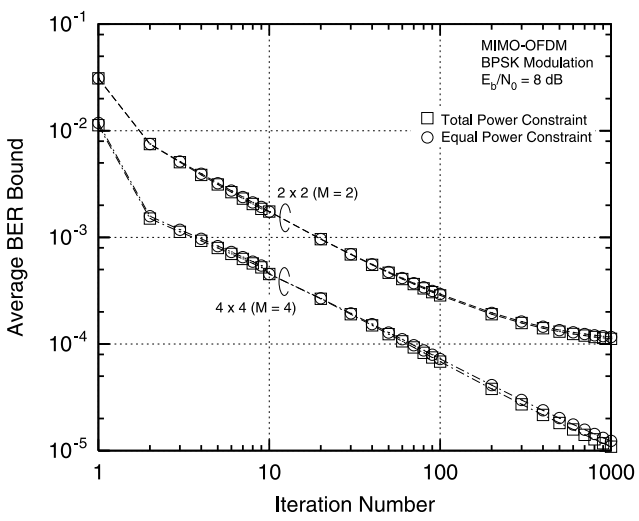

(a) Convergence characteristics

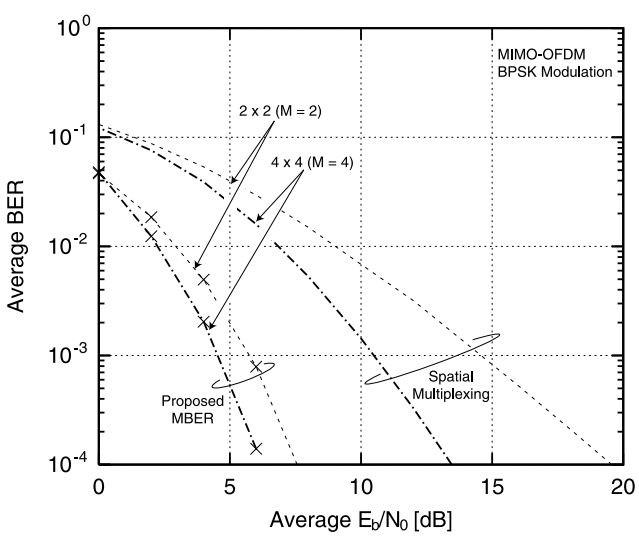

(b) Average BER performances

Fig. 9 2×2 and 4×4 MIMO-OFDM systems with BPSK.

4.5 Extended Applications of MBER

4.5.1 4×4 MIMO-OFDM with BPSK

Figure 9 shows (a) the convergence characteristics and (b) the average BER performances of the 2×2 and 4×4 MIMO-OFDM systems with BPSK modulation. Note that the equal power precoding matrix initialization with the fixed step size were employed. The number of independent data streams, M, was set to 2 and 4 for the 2×2 and 4×4 systems, respectively. The maximum number of iterations was $1,000$.

The convergence properties in Fig. 9(a) show that the total transmit power constraint provides slightly better convergence characteristic than the equal transmit power constraint when the number of transmit-receive antenna increases. This is because the strictness of the equal transmit power constraint that prohibits the transfer of transmit power between antennas becomes more influential when the number of transmit antennas increases. It is also noteworthy that while the 2×2 system saturates with iteration number greater than 800, the 4×4 system does not exhibit such behavior. This implies that with a large number of transmit antennas, more iterations are required for the steepest descent algorithm to sufficiently converge. For mitigating this problem, other numerical algorithms can be applied to accelerate convergence or the correlation between adjacent subcarrier channels can be exploited to reduce the number of precoding matrices to be obtained.

The BER performances of the 2×2 and 4×4 systems are shown in Fig. 9(b). It can be seen that the proposed precoding method can improve BER of both the 2×2 and 4×4 MIMO systems. However, the improvement in E_b/N_0 of the 4×4 system is less than that of the 2×2 system. This is because a larger number of independent data streams in the 4×4 system leads to a more densely packed signal constellation, which limits the ability to manipulate the Euclidean distance of the precoder.

4.5.2 16QAM for 2×2 MIMO-OFDM

Figure 10 shows (a) the convergence characteristic and (b) the average BER performance of the 2×2 MIMO-OFDM system with 16QAM modulation. Figure 10(a) shows that the steepest descent algorithm sufficiently converges at the iteration number greater than 100. Therefore, the average BER evaluation in Fig. 10(b) set the maximum number of iterations to 100. It is found that the proposed MBER precoder can provide an improvement of about 5 dB in the average E_b/N_0 over the spatial multiplexing at BER = 10^{-3}. Note that this improvement is less than the QPSK modulation because the constellation of 16QAM is more complex and makes it more difficult to optimize the Euclidean distances.

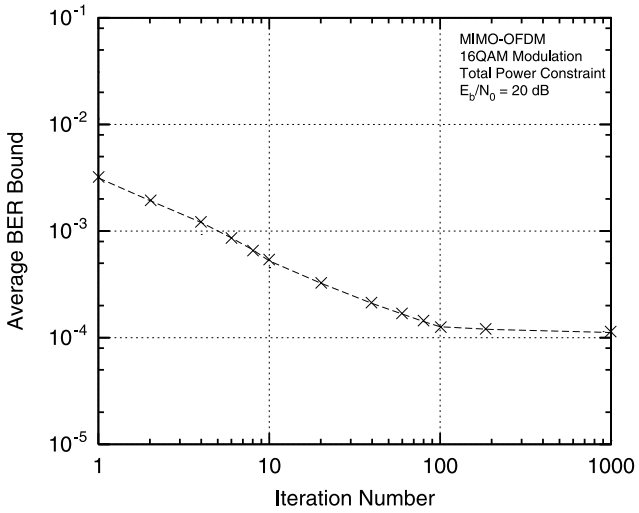

(a) Convergence characteristic

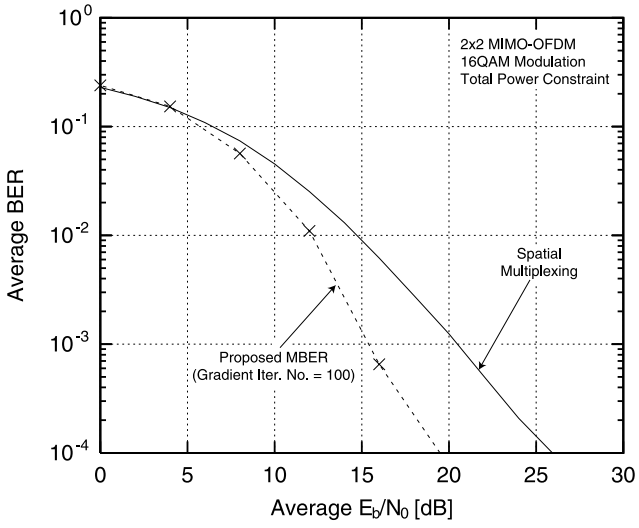

(b) Average BER Performance

Fig. 10 2×2 MIMO-OFDM systems with 16QAM.

5. Conclusions

This paper has proposed a minimum BER (MBER) precoder for a MIMO-OFDM system employing MLD. The proposed method controls the precoding matrices so that they can minimize an upper bound of BER derived from the pairwise error under two power constraints; the total power and equal transmit power constraints. The gradient algorithm is applied to this optimization problem.

Computer simulations demonstrated that the proposed precoding method for the QPSK modulation is much superior to the MMSE, the minimum distance-based, and the conventional MBER precoders in BER performance. Other aspects of the procoding were also investigated such as the distribution of BER among subcarriers, the signal constellations, and the outage probability. Finally, the simulation with a higher modulation scheme such as 16QAM clarified that the proposed MBER precoder can improve the average BER similarly.

References

[1] G.J. Foschini, "Layered space-time architecture for wireless communication in a fading environment when using multi-element antennas," Bell Labs. Tech. J., vol.1, no.2, pp.41–59, 1996.

[2] E. Teletar, "Capacity of multi-antenna Gaussian channels," Bell Labs. Tech. Rep., June 1995.

[3] H. Sampath, P. Stoica, and A. Paulraj, "Generalized linear precoder and decoder design for MIMO channels using the weighted MMSE criterion," IEEE Trans. Commun., vol.49, no.12, pp.2198–2206, Dec. 2001.

[4] S.S. Chan, T.N. Davidson, and K.M. Wong, "Asymptotically minimum BER linear block precoders for MMSE equalisation," IEE Proc., Commun., vol.151, pp.297–304, Aug. 2004.

[5] A. Hjorungnes, P.S.R. Diniz, and M.L.R. de Campos, "Jointly minimum BER transmitter and receiver FIR MIMO filters for binary signal vectors," IEEE Trans. Signal Process., vol.52, no.4, pp.1021–1036, April 2004.

[6] A. Hjorungnes and P.S.R. Diniz, "Minimum BER prefilter transform for communications systems with binary signaling and known FIR MIMO channel," IEEE Trans. Signal Process., vol.12, no.3, pp.234–237, March 2005.

[7] D.P. Palomar, M. Bengtsson, and B. Ottersten, "Minimum BER linear transceivers for MIMO channels via primal decomposition," IEEE Trans. Signal Process., vol.53, no.8, pp.2866–2882, Aug. 2005.

[8] Z. Yan, K.M. Wong, and J. Zhang, "Minimum BER power allocation for V-BLAST detected MIMO system," ISSPIT, pp.70–73, Dec. 2003.

[9] Z. Yan, K.M. Wong, and Z. Luo, "Optimal diagonal precoder for multiantenna communication systems," IEEE Trans. Signal Process., vol.53, no.6, pp.2089–2100, June 2005.

[10] A. Scaglione, P. Stoica, S. Barbarossa, G.B. Giannakis, and H. Sampath, "Optimal designs for space-time linear precoders and decoders," IEEE Trans. Signal Process., vol.50, no.5, pp.1051–1064, May 2002.

[11] P. Rostaing, O. Berder, G. Burel, and L. Collin, "Minimum BER diagonal precoder for MIMO digital transmissions," Signal Process., vol.82, pp.1477–1480, Oct. 2002.

[12] L. Collin, O. Berder, P. Rostaing, and G. Burel, "Optimal minimum distance-based precoder for MIMO spatial multiplexing systems," IEEE Trans. Signal Process., vol.52, no.3, pp.617–627, March 2004.

[13] P. Stoica and G.A. Ganesan, "Maximum-SNR spatial-temporal formatting designs for MIMO channels," IEEE Trans. Signal Process., vol.50, no.12, pp.3036–3042, Dec. 2002.

[14] F. Rey, M. Lamarca, and G. Vazquez, "Robust power allocation algorithms for MIMO OFDM systems with imperfect CSI," IEEE Trans. Signal Process., vol.53, no.3, pp.1070–1085, March 2005.

[15] G. Jongren, M. Skoglund, and B. Ottersten, "Combining beamforming and orthogonal space-time block coding," IEEE Trans. Inf. Theory, vol.48, no.3, pp.611–627, March 2002.

[16] A. Narula, M.J. Lopez, M.D. Trott, and G.W. Wornell, "Efficient use of side information in multiple-antenna data transmission over fading channels," IEEE J. Sel. Areas Commun., vol.16, no.8, pp.1423–1436, Oct. 1998.

[17] E.N. Onggosanusi, A.M. Sayeed, and B.D.V. Veen, "Optimal antenna diversity signaling for wide-band systems utilizing channel side information," IEEE Trans. Commun., vol.50, no.2, pp.341–353, Feb. 2002.

[18] A. Wittneben, "Optimal predictive Tx combining diversity in correlated fading for microcellular mobile radio applications," IEEE GLOBECOM'95, pp.48–54, Nov. 1995.

[19] R. Negi, A.M. Tehrani, and J. Cioffi, "Adaptive antennas for space-

time coding over block-time invariant multipath fading channels," IEEE VTC99, vol.1, pp.70–74, May 1999.
[20] H. Sampath and A. Paulraj, "Linear precoding for space-time coded systems with known fading correlations," IEEE Commun. Lett., vol.6, no.6, pp.239–241, June 2002.
[21] S. Chen, N.N. Ahmad, and L. Hanzo, "Adaptive minimum bit-error rate beamforming," IEEE Trans. Wireless Commun., vol.4, pp.341–348, March 2005.
[22] S. Haykin, Adaptive Filter Theory, 3rd ed., Prentice Hall 1996.
[23] C. Douillard, M. Jeźeźquel, and C. Berrou, "Iterative correction of intersymbol interference: Turbo-equalization," European Trans. Telecommun., vol.6, no.5, pp.507–511, Sept.-Oct. 1995.
[24] IEEE Std 802.11a, High-speed Physical Layer in the 5 GHz Band, 1999.

Appendix A: Conjugate Derivative of $J_e(\mathbf{F}(n))$

From (30), the conjugate derivative of $J_e(\mathbf{F}(n))$ can be written as

$$\left[\frac{\partial J_e(\mathbf{F}(n))}{\partial \mathbf{F}^*(n)}\right]_{km} = \frac{\partial J_e(\mathbf{F}(n))}{\partial F^*_{km}(n)} = \sum_{\tilde{b}}\sum_{\tilde{c}\neq\tilde{b}} N_e(\tilde{b}\to\tilde{c})\frac{\partial}{\partial F^*_{km}(n)}\mathrm{erfc}\sqrt{\gamma(\tilde{b}\to\tilde{c})}. \quad (\mathrm{A}\cdot 1)$$

Since the complementary error function is defined as

$$\mathrm{erfc}(x) = \frac{2}{\sqrt{\pi}}\int_x^\infty e^{-t^2}\,dt, \quad (\mathrm{A}\cdot 2)$$

the conjugate derivative in (A· 1) becomes

$$\begin{aligned}\frac{\partial}{\partial F^*_{km}(n)}\mathrm{erfc}\sqrt{\gamma(\tilde{b}\to\tilde{c})} &= -\frac{1}{\sqrt{\pi}}[\exp(-\gamma(\tilde{b}\to\tilde{c}))] \\ &\quad\times[\gamma(\tilde{b}\to\tilde{c})]^{-1/2}\frac{\partial}{\partial F^*_{km}(n)}\gamma(\tilde{b}\to\tilde{c}) \\ &= -\frac{1}{4\sqrt{\pi}\sigma_N^2}[\gamma(\tilde{b}\to\tilde{c})]^{-1/2}[\exp(-\gamma(\tilde{b}\to\tilde{c}))] \\ &\quad\times\frac{\partial}{\partial F^*_{km}(n)}\mathrm{tr}\{\mathbf{H}(n)\mathbf{F}(n)\mathbf{A}(\tilde{b}\to\tilde{c}) \\ &\quad\times\mathbf{F}^{\mathrm{H}}(n)\mathbf{H}^{\mathrm{H}}(n)\},\end{aligned} \quad (\mathrm{A}\cdot 3)$$

where the definitions of (17), (22), and (32) were used. The conjugate derivative in (A· 3) can be rewritten as

$$\begin{aligned}&\frac{\partial}{\partial F^*_{km}(n)}\mathrm{tr}\{\mathbf{H}(n)\mathbf{F}(n)\mathbf{A}(\tilde{b}\to\tilde{c})\mathbf{F}^{\mathrm{H}}(n)\mathbf{H}^{\mathrm{H}}(n)\} \\ &= \frac{\partial}{\partial F^*_{km}(n)}\mathrm{tr}\{\mathbf{H}^{\mathrm{H}}(n)\mathbf{H}(n)\mathbf{F}(n)\mathbf{A}(\tilde{b}\to\tilde{c})\mathbf{F}^{\mathrm{H}}(n)\} \\ &= \frac{\partial}{\partial F^*_{km}(n)}\sum_{k'=1}^{N_T}\sum_{m'=1}^{M}[\mathbf{H}^{\mathrm{H}}(n)\mathbf{H}(n)\mathbf{F}(n)\mathbf{A}(\tilde{b}\to\tilde{c})]_{k'm'} \\ &\quad\times F^*_{k'm'}(n) \\ &= [\mathbf{H}^{\mathrm{H}}(n)\mathbf{H}(n)\mathbf{F}(n)\mathbf{A}(\tilde{b}\to\tilde{c})]_{km}.\end{aligned} \quad (\mathrm{A}\cdot 4)$$

Substituting (A· 3) and (A· 4) into (A· 1) yields

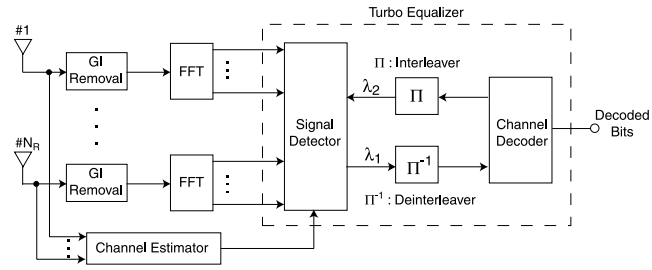

Fig. A· 1 MIMO-OFDM receiver employing turbo equalizer.

$$\begin{aligned}\left[\frac{\partial J_e(\mathbf{F}(n))}{\partial \mathbf{F}^*(n)}\right]_{km} &= -\frac{1}{4\sqrt{\pi}\sigma_N^2} \\ &\quad\times\sum_{\tilde{b}}\sum_{\tilde{c}\neq\tilde{b}} N_e(\tilde{b}\to\tilde{c})[\gamma(\tilde{b}\to\tilde{c})]^{-1/2}\exp[-\gamma(\tilde{b}\to\tilde{c})] \\ &\quad\times[\mathbf{H}^{\mathrm{H}}(n)\mathbf{H}(n)\mathbf{F}(n)\mathbf{A}(\tilde{b}\to\tilde{c})]_{km}.\end{aligned} \quad (\mathrm{A}\cdot 5)$$

Appendix B: Turbo Equalization

Figure A· 1 shows a block diagram of the MIMO-OFDM receiver employing the turbo equalizer. The turbo equalizer iterates signal detection and channel decoding by exchanging log likelihood ratio (LLR) of coded bits denoted by λ_1 and λ_2, respectively. Since the proposed method can improve the BER performance of the signal detector such as MLD, λ_1 becomes more reliable. Using more accurate λ_1, the channel decoder performs the decoding and can provide more accurate LLR λ_2. Thus, the proposed method is expected to improve the BER performance of the turbo equalization.

Boonsarn Pitakdumrongkija received the B.S. degree from Sirindhorn International Institute of Technology Thammasat University, Thailand in 2002 and the M.S. degree from Tokyo Institute of Technology, Japan in 2005. Currently, he is working towards the Dr.Eng. degree in Communications and Integrated Systems Dept. at Tokyo Institute of Technology, Tokyo, Japan. His research areas include signal processing technique for mobile communications.

Kazuhiko Fukawa received the B.S. and M.S. degrees in physics, and the Dr. Eng. degree in electrical and electronics engineering, all from Tokyo Institute of Technology, Tokyo, Japan, in 1985, 1987, and 1999 respectively. He joined Nippon Telegraph and Telephone Corporation (NTT), Japan, in 1987. Since then, he has been engaged in research on digital mobile radio communication systems and applications of the adaptive signal processing, including adaptive equalization, interference cancellation, and adaptive arrays. He was a Senior Research Engineer at NTT Mobile Communications Network Inc. (NTT DoCoMo), from 1994 to 2000. Since April 2000, he has been an Associate Professor at the Tokyo Institute of Technology. Dr. Fukawa is a member of IEEE. He received the Paper Award from IEICE in 1995 and 2007.

Hiroshi Suzuki received the B.S. degree in electrical engineering, the M.S. degree in physical electronics, and the Dr.Eng. Degree in electrical and electronics engineering, all from the Tokyo Institute of Technology, Tokyo, in 1972, 1974, and 1986, respectively. He joined the Electrical Communication Laboratories, Nippon Telegraph and Telephone Corporation (NTT), Japan, in 1974. He was engaged in research on devices in millimeter-wave regions. Since 1978, he has been engaged in fundamental and developmental researchers on digital mobile communication systems. He was an Executive Research Engineer in the Research and Development Department, NTT Mobile Communications Network, Inc. (NTT DoCoMo) from 1992 to 1996. Since September 1996, he has been a Professor at the Tokyo Institute of Technology. He is currently interested in various applications of the adaptive signal processing to radio signal transmission: adaptive arrays, multiuser detection, interference canceling, and MIMO-OFDM for future advanced multiple access communication systems. Dr. Suzuki is a member of IEEE. He received the Paper Award from the IEICE in 1995 and 2007, and the award of IEICE Fellow in 2006.

Takashi Hagiwara received the B.S. and M.S. degree from Tokyo Institute of Technology, Japan in 2004 and 2006, respectively. Currently, he is interested in various applications of the adaptive signal processing to digital radio communication systems including interference canceling and adaptive equalization.